Noise and critical behavior of the pupil light reflex at oscillation onset

André Longtin*
Department of Physics, Rutherford Physics Building, McGill University, 3600 University, Montréal, Québec, Canada H3A 2T8

John G. Milton†
Department of Physiology, McIntyre Medical Sciences Building, McGill University, 3655 Drummond, Montréal, Québec, Canada H3G 1Y6

Jelte E. Bos
Department of Medical Physics, Faculty of Medicine, Free University, 1081 BT Amsterdam, The Netherlands

Michael C. Mackey
Department of Physiology, Department of Physics, and Center for Nonlinear Dynamics in Medicine and Physiology, McGill University, 3655 Drummond, Montréal, Québec, Canada H3G 1Y6

(Received 28 November 1989)

We have induced oscillations in the human pupil light reflex using two different kinds of external electronic feedback: smooth negative feedback (SNF) and piecewise constant negative feedback (PCNF). The behavior of the mean amplitude and period at oscillation onset are shown to be in good agreement with a model of this neural system incorporating the external feedback. The critical behavior displayed through amplitude and period fluctuations is different in each case. The observation that amplitude fluctuations are larger (smaller) than period fluctuations for SNF (PCNF) is explained theoretically and by numerical integration of a stochastic delay-differential equation with additive and multiplicative colored noise. We find that both types of noise postpone the Hopf bifurcation in SNF by an amount proportional to the noise intensity and inversely proportional to the correlation time. The implications for analyzing bifurcations in neural systems are discussed.

I. INTRODUCTION

Oscillations occur in a wide variety of neurophysiological control systems under normal and pathological conditions.[1-3] Experimental and theoretical investigation of the properties of these oscillations from the point of view of nonlinear dynamics has been hindered by (1) the scarcity of suitable systems in which parameters can be manipulated; and (2) the presence of high-amplitude noise. Thus it has been difficult to untangle the deterministic and stochastic processes which shape the observed dynamics.

As a paradigm for neurological control systems, the human pupil light reflex exhibits oscillatory phenomena of varying complexity.[4,5] For example, regular oscillations in the pupil area occur when the gain of the feedback loop is sufficiently high,[6] and aperiodic oscillations in the pupil area occur spontaneously (a phenomenon known as "hippus"[7]). There have been studies[8] of the behavior of hippus as a function of light level and of its interaction with pupil oscillations produced by sinusoidally varying light stimuli. These have concluded that many properties of hippus can be explained by assuming that it represents multiplicative Gaussian white noise injected into the reflex at the level of the brainstem nuclei. However, the precise origin and nature of hippus are still not known, and new experimental paradigms, such as the one presented in this paper, are needed to deepen our understanding of its properties.

One advantage of studying the pupil light reflex is that it can be easily and noninvasively monitored. A second advantage is the ease with which the feedback loop can be opened[9] (i.e., the effect of the output on the input can be removed). This has led to extensive studies of the linear and nonlinear properties of the reflex components and of the noise under open loop conditions (see Ref. 5 for a review). Finally, closed-loop oscillations can be studied using an experimental setup in which the normal feedback is replaced by controllable external electronic feedback.[10] This "clamping" method produces a hybrid system in which autonomous oscillations and bifurcations can be produced and studied as a function of the control parameters.[10-13]

Recently, it has been shown[4,14] that autonomous oscillations in the normal pupil light reflex can be modeled using the nonlinear delay-differential equation (DDE)

$$\frac{dg}{dA}\frac{dA(t)}{dt}+\alpha g(A(t))=F(\bar{\phi},\phi(t-\tau)) . \quad (1)$$

Here $A(t)$ is the pupil area, $g(A)$ is a monotonically decreasing nonlinear function relating iris muscle activity to pupil area, τ is the total time delay in the system, α is related to the rate constant for pupillary movements, ϕ is the retinal light flux (equal to the product of light intensity and pupil area), and $\bar{\phi}$ is the light flux below which no response occurs. For the intact pupil light reflex with

negative feedback,

$$F(\bar{\phi},\phi(t-\tau))=\gamma \ln\left[\frac{\phi(t-\tau)}{\bar{\phi}}\right], \tag{2}$$

where γ is a physiological parameter related to the transduction of light intensity into neural firing frequency in the optic nerve and the midbrain. The model also takes into account the logarithmic compression of light fluxes in the transduction process at the retina.

In this paper we study the noisy behavior of the period and the amplitude of oscillations induced in the human pupil light reflex by replacing the function F with two kinds of external feedback: (1) piecewise constant negative feedback (PCNF) [Fig. 1(a)]; and (2) smooth (i.e., differentiable) negative feedback (SNF) [Fig. 1(b)]. Equations (1) and (2) contain many parameters which are difficult to estimate experimentally. A simpler model for SNF oscillations which displays the same qualitative behavior as Eq. (1) with F given by Eq. (2) is obtained[4] by replacing F with a Hill-type function [Fig. 1(b)] and by making $g(A)$ a linear function of A:

$$\frac{dA(t)}{dt}+\alpha A(t)=\frac{c\theta^n}{\theta^n+A^n(t-\tau)}+k\ . \tag{3}$$

This equation has been used as a paradigm for smooth negative feedback systems with delay[1] (more complicated oscillations and chaos arise when the Hill's function is nonmonotonic, i.e., in the presence of "mixed feedback;" see Ref. 1). Equation (3) exhibits a supercritical Hopf bifurcation as the parameter n or τ is increased past a certain value. In the PCNF case, we linearize $g(A)$ and take F to be piecewise constant so that (1) is replaced by the piecewise linear DDE[4,11]

$$\alpha^{-1}\frac{dA}{dt}+A(t)=\begin{cases}A_{\text{off}}, & A(t-\tau)<\theta\\ A_{\text{on}}, & A(t-\tau)>\theta\end{cases} \tag{4}$$

where A_{off} and A_{on} are constants. All the parameters in Eq. (4) can be precisely estimated from the data and the resulting oscillatory solutions have been shown to be in good agreement with the observed oscillations.[3,11,13] Further, besides being important clinically, PCNF allows certain nonlinearities of the reflex to be isolated for study.[4,13]

Specifically we examine the onset of oscillation with SNF and PCNF and look at how the period and amplitude vary as a function of gain (SNF) and threshold (PCNF). As the Hopf bifurcation is approached (in the SNF case), critical slowing down occurs, i.e., the decay time of perturbations increases which leads to noise amplification. We find that the critical behavior at oscillation onset, manifested in period and amplitude fluctuations, is interesting and different in each case. We show that theoretical and numerical analysis of simple stochastic DDE's can explain this behavior. We are not aware of any previous studies of the interaction of noise with autonomous oscillations in either the pupil light reflex or any other neural reflex. Thus our study provides insight into the origins and effect of noise in neural systems, as well as the effect of noise on solutions of DDE's. These results are of interest since physiological systems are inherently noisy and the transition from equilibrium to dynamic behavior is frequently encountered.[1-3]

The experimental method is described in Sec. II. In Sec. III we present the experimental results for both the SNF and PCNF cases. Section IV is devoted to a theoretical and numerical analysis of the deterministic and stochastic behaviors of amplitude and period for both cases. The transition from SNF to PCNF is the subject of Sec. V. The paper concludes with a discussion in Sec. VI.

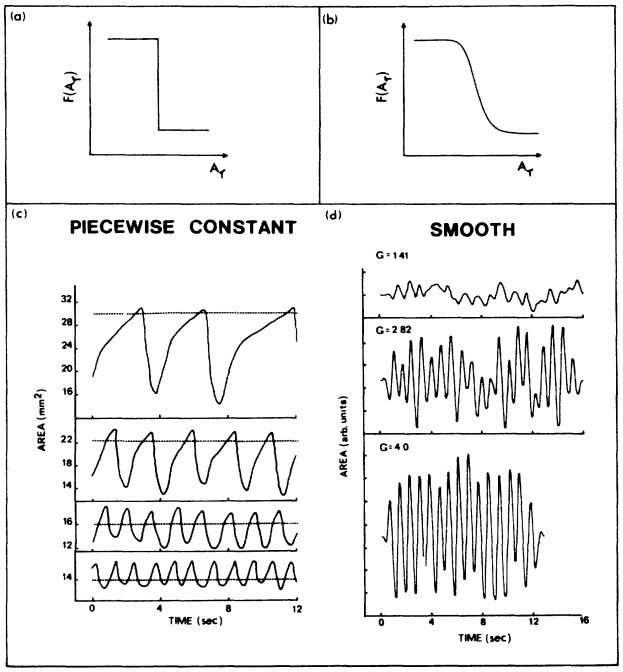

FIG. 1. Pupil area oscillations induced using (a) external piecewise constant negative feedback (PCNF), and (b) smooth negative feedback (SNF). The PCNF oscillations in (c), measured using an infrared videopupillometer, were obtained for the following area threshold values (dotted line): 30.1 mm^2 (upper panel), 22.5 mm^2, 16.2 mm^2, and 14.0 mm^2. The SNF oscillations in (d) are obtained for increasing values of the feedback gain [proportional to the slope in (b)]. Oscillation onset occurs at $G\simeq 1$. The SNF oscillations were measured using a reflectance technique which does not allow calibration in absolute units of area. Correcting for baseline drift in SNF by linear trend subtraction produced 12–15-sec long data sets. The PCNF oscillations did not exhibit baseline drift.

II. EXPERIMENTAL METHODS

A. Background

The pupil light reflex is a negative feedback neurological control system which regulates the light flux falling on the retina [ϕ in Eq. (1)] to within a certain range. An increase in retinal light flux due to an increase in light intensity is compensated by a decrease in flux due to pupil

constriction, and *vice versa*. This constriction results from the increase in neural activity to the iris sphincter (constrictor) muscle (in the colored part of the eye), which is proportional to the logarithm of the light flux. During pupil cycling, dilation is thought to be primarily due to passive relaxation of the sphincter muscle and to inhibition of the neural activity to this muscle.[4] This describes "closed-loop" operation under normal smooth negative feedback conditions.

The feedback loop can be opened using illumination in Maxwellian view,[9] i.e., by focusing a narrow beam of light down the center of the pupil. The diameter of this beam is so small that the iris can never shade the retina from the beam. Under these conditions, the pupil response has no influence on retinal light flux.

The idea behind clamping the pupil light reflex is to electronically control the intensity of a light source (in Maxwellian view) using an analog signal proportional to pupil area (provided by a pupillometer). For example, one can choose to synthesize the naturally occurring negative feedback characteristic. This involves clamping the pupil light reflex using a linear amplifier with controllable positive gain to convert area variations into light intensity variations.[10,12] From the point of view of pupil area, this corresponds to negative feedback because of the inverse relationship between pupil area and light intensity. The retinal flux variations are then given by the product of this varying light intensity and the fixed beam area.

When the electronic feedback comprises such a linear amplifier, the pupil area exhibits limit cycle oscillations. This is possible only if nonlinearities in the reflex constrain the amplitude of the oscillation. In the SNF case,[4] the effective feedback in the whole circuit can be modeled by Eq. (3) in which the feedback on the right-hand side is described by a sigmoidal curve as in Fig. 1(b). In other words, the linear amplifier contributes to the steep slope in Fig. 1(b), while pupil nonlinearities are responsible for the saturation at high and low area values. In the PCNF case the effective feedback is as shown in Fig. 1(a). While the oscillations obtained in the SNF case are often difficult to control due to drifts in mean pupil area,[10,12] those obtained in the PCNF case are relatively more stable.[11,13]

An infrared videopupillography technique[11] was used for the PCNF study while a reflectance technique[12] was used for the SNF study, as a result of the collaboration between the authors. While each method has its advantages, they are both efficient recording techniques with high enough sampling rate and accuracy for the proper assessment of the phenomena presented here. Hence our results are not a consequence of the different pupil area measuring techniques for SNF and PCNF.

B. Piecewise constant negative feedback

The experimental method has been described previously.[11] The 1.2-mm-diam light beam used for open-loop illumination was provided by a 605-nm peak wavelength light-emitting diode (LED). The retinal illumination provided by the light beam was fixed at a value of 750 trolands. Subjects were dark adapted for at least 15 min in a room lit by a dim red light; this was the background illumination for the experiment. The analog output of an infrared binocular videopupillometer (Hamamatsu Iriscorder Model C-2515, sampling rate 60 Hz), which is proportional to pupil area, was electronically compared to an adjustable area threshold θ. Through this area comparator [Fig. 1(a)], the state of the system, i.e., pupil area $A(t)$, controls the timing and duration of the light pulses. The light is turned on whenever $A > \theta$. The linearity of area measurement is better than 1% from 0 to 150 mm^2 with an accuracy of 0.01 mm^2. Pupil responses to light changes are not instantaneous. They follow a neural delay of $\approx$300 msec (approximately the same for light onset and offset[13]) plus a 100-msec delay due to electronic processing. In all experiments the pupil being measured was also the one being stimulated.

C. Smooth negative feedback

The pupillometer used for the SNF experiments is based on an infrared reflectance technique which has been described previously.[12] It yields a relative measure of pupil size which is linearly related to pupil area. Infrared emitters and detectors are mounted in units attached to a head band and are positioned approximately 3 cm in front of both eyes. The light stimulus for SNF was provided by a small yellow (583-nm peak wavelength) LED which illuminates the retina in Maxwellian view by means of two lenses. The retina is centrally illuminated with a circular field approximately 30° wide. In between the two lenses, a fixation target is mounted. In order to prevent the visible light of the stimulus LED from adding to the signal from the infrared detectors, the stimulus LED current and the infrared detection are pulsed out of phase at 4000 Hz. The retinal illuminance was typically adjusted between 500 and 1000 trolands.

The SNF was synthesized using a linear amplifier relating the analog pupil area signal to the stimulus LED current. No significant delay was introduced by the external feedback. The offset and the gain of the amplifier were adjusted by the experimenter. Signals representing pupil area together with a calibrated signal related to stimulus intensity were recorded digitally at a sampling rate of 50 Hz. Because of very slow noisy fluctuations in the pupillary system, the mean light intensity cannot control the mean pupil area, which leads to baseline drift. Correcting for baseline drift by linear trend subtraction produced 12–15-sec-long data sets. The pupil being measured was also the one being stimulated.

III. EXPERIMENTAL RESULTS

A. Piecewise constant negative feedback

Figure 1(c) shows typical time series of PCNF-induced pupillary oscillations for different area threshold (θ) values. We restricted our attention to values of θ that produce an oscillation (i.e., $\theta < A_{\text{off}}$). The oscillations have one maximum per period. The power spectra for these oscillations are shown in Figs. 2(a)–2(c). The high threshold oscillations have a richer harmonic content

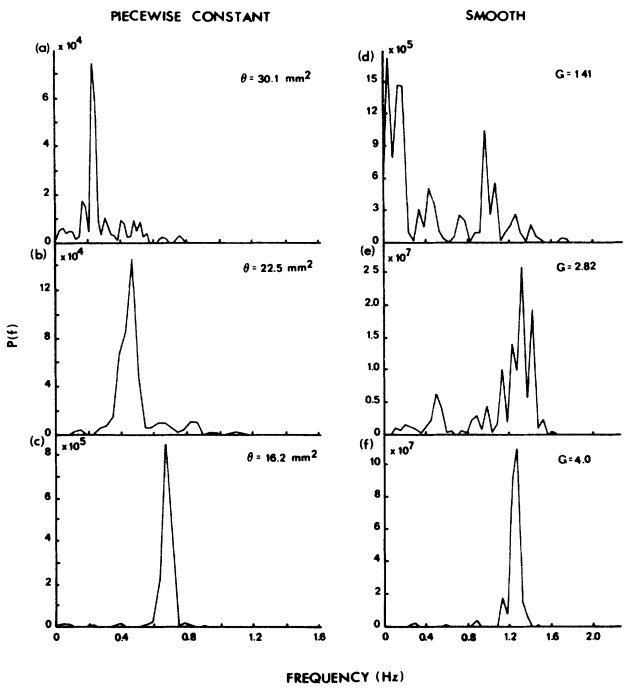

FIG. 2. (a) Power spectra of pupil oscillations shown in Fig. 1. For PCNF (a)–(c) the spectra were obtained by running a fast-Fourier transform (FFT) on Parzen-windowed data resampled at 20 Hz. Note the shift in the dominant peak as the threshold changes. For SNF (d)–(f), the spectra were obtained by performing a FFT on the data. As the gain increases, low-frequency peaks disappear as the power becomes concentrated in the dominant peak.

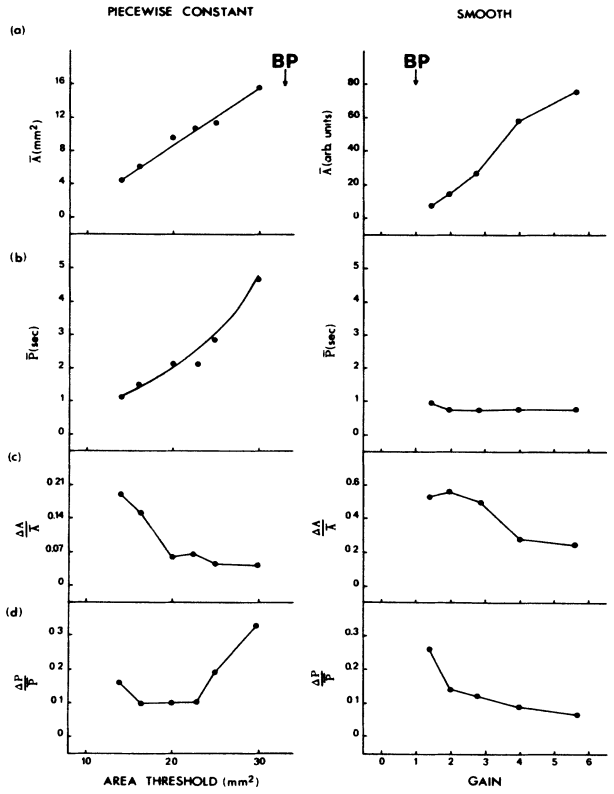

FIG. 3. Means and fluctuations of oscillation amplitude and period as a function of threshold (PCNF) and gain (SNF). Oscillation onset occurs at the threshold or gain value marked bifurcation point (BP). Oscillations occur to the left of BP for PCNF and to its right for SNF. (a) Mean amplitude $\bar{A}$; (b) mean period $\bar{P}$; (c) relative amplitude $\Delta A/\bar{A}$ fluctuations; (d) relative period $\Delta P/\bar{P}$ fluctuations. The fluctuations ΔA and ΔP are the standard deviations of the means $\bar{A}$ and $\bar{P}$ at corresponding gain or threshold settings. The PCNF data were obtained from one subject (to minimize variability) by measuring pupil area for $\approx$20–25 sec at each threshold setting. The SNF data were also obtained from a single (but different) subject. At each gain setting, area was measured during 2–3 runs totaling $\approx$40 sec. Amplitudes were measured from peak to trough, while periods were measured as the time between successive peaks. Note that $\Delta A/\bar{A}$ is larger for SNF than for PCNF and larger than $\Delta P/\bar{P}$ in SNF. Also, $\Delta P/\bar{P}$ is larger in PCNF than in SNF and larger than $\Delta A/\bar{A}$ in PCNF.

than the lower threshold ones which are nearly sinusoidal. Also, the spectra show little power below the fundamental frequency. The oscillation waveforms in PCNF have no particular symmetry that would be reflected in the power spectra (such as a square wave). In fact, the waveform is clearly asymmetric, especially at high threshold. This is due to the fact that constriction is faster than dilation.[11,13] This asymmetry is highlighted by transient responses to light steps as occurs in PCNF, and not by responses to the continuously varying light intensity as occurs in SNF.[4,14]

In Figs. 3(a)–3(b) we have plotted the mean oscillation amplitude $\bar{A}$ and period $\bar{P}$ as a function of θ. Note that the bifurcation point (BP) corresponding to oscillation onset is to the right of the figure. When $A_{\text{off}} < \theta$ the pupil is in an equilibrium state characterized by less than 5% fluctuations around the mean pupil area (low-amplitude hippus occurring at large pupil areas). When $A_{\text{off}} > \theta$, a transition occurs between this state and an oscillatory state. $\bar{P}$ and $\bar{A}$ are monotonically increasing functions of θ.

In Figs. 3(c) and 3(d) we plot the relative amplitude and period fluctuations ($\Delta A/\bar{A}$ and $\Delta P/\bar{P}$, respectively) for the same range of thresholds. ΔA does not vary much over the range of θ values. Since $\bar{A}$ increases as the bifurcation point is approached (i.e., as θ increases), $\Delta A/\bar{A}$ will decrease. However, ΔP increases as θ increases. Further, ΔP increases faster than $\bar{P}$, yielding a value of $\Delta P/\bar{P}$ that increases with θ. We would obtain the same result if, instead of $\Delta P/\bar{P}$, we plotted $\Delta f/\bar{f}$ where $f = 1/P$ is the oscillation frequency. In fact, at higher thresholds the power spectra have a high background, especially in the 0.1–0.5-Hz range, and the peak of the fundamental mode has less power as the bifurcation point is approached.

B. Smooth negative feedback

Figures 1(d) and 2(d)–2(f), respectively, show time series of the oscillations in pupil area that occur with SNF and the corresponding power spectra. The oscillations have a nearly sinusoidal shape with a fluctuating amplitude and period. In fact, the spectra for the higher gains area dominated by the fundamental mode (1.1–1.3 Hz), and there is little harmonic content. At the lower gain setting [Fig. 2(d)] there is a more pronounced 0.1–0.2-Hz rhythm in addition to the fundamental mode. The data set length is limited by saturation of the area signal which results in a clipped oscillation (not shown). These saturations appear to be due to uncontrollable baseline (mean area) drift which in turn is caused by pupillary noise. These oscillations, as well as those for PCNF, were found to not be significantly affected by blinking. Also, in contrast to those for the PCNF case, the waveforms are symmetric.

The mean amplitude and mean period of the SNF oscillations are plotted as a function of the feedback gain G in Figs. 3(a) and 3(b). The gain has been normalized such that $G \simeq 1$ when the pupil starts to oscillate. In this case the bifurcation point is at the left of the figure, and the oscillations become more prominent as the gain is increased. $\bar{A}$ increases with G in a roughly sigmoidal fashion. Over the same range of gain values, $\bar{P}$ is quite constant but there are relatively larger fluctuations at small G values.

The relative fluctuations in amplitude and period are plotted in Figs. 3(c) and 3(d) for the range of gain values studied. Amplitudes are measured as peak-to-trough differences, while periods are measured as the time between successive peaks. $\Delta A/\bar{A}$ is larger than $\Delta P/\bar{P}$ over this whole range. However, both increase rapidly at lower gains, reaching values of $\Delta A/\bar{A} \sim 0.5$ and $\Delta P/\bar{P} \sim 0.2$. At higher gains, these values level off at $\Delta A/\bar{A} \sim 0.2$ for amplitude and $\Delta P/\bar{P} \sim 0.05$ for the period.

The spectra in Figs. 2(d)–2(f) show that there is considerable power below the fundamental frequency. This reflects the baseline and amplitude fluctuations within each data set. These fluctuations also make ambiguous the determination of the point of oscillation onset by extrapolation to zero amplitude. The spectra show that the noise is more prominent around 0.5 Hz, and that its bandwidth does not seem to exceed 1 Hz. This implies that the correlation time of these fluctuations is on the order of 1–2 sec (reciprocal of the low-frequency noise bandwidth). This is in agreement with previous studies which indicate that the spectrum of noise in open loop is quasiwhite up to a cutoff frequency of $\simeq 0.5$ Hz.[7,8] In fact, high-frequency noise (observable up to ~ 25 Hz by Nyquist's criterion) is very small, and inspection of the oscillations reveals that they are smooth. Previous investigations[10] have shown that autonomous oscillations exhibit less high-frequency noise than those obtained using, e.g., external periodic forcing. This has been explained by the fact that the autonomous system behaves like a resonant low-pass filter when it oscillates.[10] However, the slower extraneous oscillations are not suppressed and are clearly apparent in our data.

IV. THEORETICAL ANALYSIS

A. Deterministic analysis

In this section we explain the deterministic results for the SNF and PCNF cases.

1. PCNF

The dynamics of PCNF-induced oscillations are governed by Eq. (4).[3,11,13] The solutions of Eq. (4) are simple increasing or decreasing exponentials, because at any given time the forcing (i.e., the right-hand side) is constant. The oscillation is bounded from above by an upper asymptote A_{off}, towards which the pupil dilates when the light is off. Likewise, when the light is on, the area tends to a lower asymptote A_{on}. Note that on crossing θ the slope of the solution does not change instantly. This is due to the finite delay (neural plus electronic) in the system. The exact shape of the observed oscillations is not reproduced by this piecewise linear model, e.g., the derivative is not continuous (at least a second-order piecewise linear model would be required). However, the model has the advantage that analytical expressions exist for the period P and amplitude $\tilde{A}$ (Refs. 4 and 13)

$$P = 2\tau + \alpha_c^{-1} \ln\left[\frac{A_{\max} - A_{\text{on}}}{\theta - A_{\text{on}}}\right] + \alpha_d^{-1} \ln\left[\frac{A_{\min} - A_{\text{off}}}{\theta - A_{\text{off}}}\right], \tag{5}$$

$$\tilde{A} = A_{\max} - A_{\min}, \tag{6}$$

where $A_{\max}$ and $A_{\min}$ are the maximum and minimum areas reached by the oscillation as it approaches, respectively, the asymptotes A_{off} and A_{on}:

$$A_{\max} = \theta e^{-\alpha_d \tau} + A_{\text{off}}(1 - e^{-\alpha_d \tau}), \tag{7}$$

$$A_{\min} = \theta e^{-\alpha_c \tau} + A_{\text{on}}(1 - e^{-\alpha_c \tau}). \tag{8}$$

Note that $A_{\text{on}} < A_{\min} < A_{\max} < A_{\text{off}}$.

Further, all parameters can be estimated experimentally:[3,13] α_d is determined from the slope and A_{off} from the intercept of the plot of $A_{\max}$ versus θ. In the same manner, $A_{\min}$ versus θ yields A_{on} and α_c. The threshold θ is set electronically, and the delay τ is measured independently from the pupil response to a single pulse of light. We have taken the response asymmetry into account by making α dependent on the area derivative, i.e., $\alpha = \alpha_c$ when $\dot{A} < 0$ (constriction), and $\alpha = \alpha_d$ otherwise. Asymmetry can be neglected in the SNF case where continuous variations in light intensity (as opposed to the abrupt changes in PCNF) emphasize steady-state rather than transient behavior, leading to an averaging of the rate constants.[14]

Equation (4) has been shown to predict the period, amplitude, and light pulse widths in the PCNF case to an accuracy of 5–10 %.[3,11,13] Equation (6) predicts that the

amplitude should be independent of θ in the symmetric case $\alpha_c=\alpha_d$, and increase linearly with θ when $\alpha_c>\alpha_d$. Our data clearly support the asymmetric case. Further, as θ is increased from low values, the period should first decrease slightly, then increase over the major portion of its range. Apart from the slight decrease in period, this behavior is observed.

2. SNF

For the SNF case, Eq. (3) has periodic solutions[1,4] when

$$\omega\tau=\cos^{-1}\left[-\frac{\alpha}{\beta}\right], \tag{9}$$

where $\omega=(\beta^2-\alpha^2)^{1/2}$ is the angular frequency of the oscillation at the bifurcation and the inverse cosine takes its value in the interval $[\pi/2,\pi]$. β is the slope of the feedback function evaluated at the fixed point $F'(A^*)$. A supercritical Hopf bifurcation occurs when $F'(A^*)$ or τ are made sufficiently large, in which case the left-hand side of Eq. (9) is greater than the right-hand side. Thus the amplitude of the limit cycle increases near the bifurcation as the square root of the distance from the bifurcation point (such as the order parameter in a second-order phase transition[15]). This amplitude behavior is roughly seen in our data [Fig. 3(a)] at higher gain. The origin of the behavior of the mean amplitude near oscillation onset will be explained in the stochastic analysis section below.

Assuming that F is given by the Hill's function in Eq. (3), it is straightforward to show that $\partial T/\partial n<0$ at the bifurcation point, where $T=2\pi/\omega$ is the oscillation period. However, numerical integration of Eq. (3) reveals that the period remains constant near the bifurcation point and increases monotonically thereafter until it reaches the value of the period analytically predicted for PCNF. This is true for different values of α; further, the period increases very slowly as α is decreased ($\alpha=3.21$, $T=0.936$; $\alpha=0.1$, $T=1.185$). This slow variation in period is observed in Fig. 3(b) except near oscillation onset where fluctuations are large. The relative constancy of the period, when compared to the amplitude, can be understood from the normal form for the Hopf bifurcation. In fact, the frequency is given by an expansion in even powers of the amplitude and hence the zeroth-order term (a constant) dominates near the bifurcation.[16]

B. Stochastic analysis

1. PCNF

The power spectra in the PCNF case have less power at low frequencies than in the SNF case [compare Figs. 2(a) and 2(d)]. These spectra are different because the two types of feedback affect the expression of the same noise sources differently. The noise in our system has a correlation time on the order of 1–2 sec (see Sec. III A). This compares well with the reports of the inverse bandwidth of the power spectra of pupil fluctuations (hippus) under constant illumination.[7,8] The response time of the pupil light reflex, which varies from 0.25 sec (constriction) to 1.5–2 sec (dilation), is of the same order. Further, the transients in Eq. (4) are very short (less than one oscillation period) due to the stability of these limit cycles. To obtain a qualitative understanding of how period and amplitude fluctuations depend on θ, we assume that the expressions for amplitude and period, based on the steady-state solution of Eq. (4), always hold. In other words, the system equilibrates to the fluctuations. We can then compute period and amplitude fluctuations by taking partial derivatives with respect to fluctuating parameters.

A previous study has shown that the asymptotes undergo cycle-to-cycle variations during PCNF oscillations.[11] The asymptotes are defined in terms of physiological parameters by[4]

$$A_{\rm off}=A_0+\frac{\gamma}{\alpha_d\beta}\ln\left[\frac{\phi_{\rm off}}{\bar{\phi}}\right], \tag{10}$$

$$A_{\rm on}=A_0+\frac{\gamma}{\alpha_c\beta}\ln\left[\frac{\phi_{\rm off}+\phi_b}{\bar{\phi}}\right], \tag{11}$$

where β is the slope of the feedback function $g(A)$ [defined in Eq. (1)] at the fixed point of Eq. (1) when F is given by Eq. (2), and A_0 is the maximum pupil area (note that $A_{\rm off}>A_{\rm on}$ since $\beta<0$). These expressions imply that if any physiological parameter fluctuates, this will affect the value of the asymptotes since they are functions of all the parameters. Furthermore, the parameter estimation scheme of Sec. IV A 1 endows the asymptotes with the largest relative error since they are obtained as intercepts of linear fits. Hence we assume that only the asymptotes fluctuate significantly, and that the asymptote, period, and amplitude fluctuations are normally distributed.[8]

Using a standard error propagation formula, the variances of the amplitude $\sigma^2_{\tilde{A}}$ and period σ^2_P are [remembering that $\tilde{A}$ is the amplitude from Eq. (6)]

$$\sigma^2_{\tilde{A}}=\left[\frac{\partial\tilde{A}}{\partial A_{\rm off}}\right]^2\sigma^2_{A_{\rm off}}+\left[\frac{\partial\tilde{A}}{\partial A_{\rm on}}\right]^2\sigma^2_{A_{\rm on}} \tag{12}$$

$$=(1-e^{-\alpha_d\tau})^2\sigma^2_{A_{\rm off}}+(1-e^{-\alpha_c\tau})^2\sigma^2_{A_{\rm on}}, \tag{13}$$

and

$$\sigma^2_P=\left[\frac{\partial P}{\partial A_{\rm off}}\right]^2\sigma^2_{A_{\rm off}}+\left[\frac{\partial P}{\partial A_{\rm on}}\right]^2\sigma^2_{A_{\rm on}}, \tag{14}$$

where

$$\frac{\partial P}{\partial A_{\rm on}}=\frac{A_{\max}-\theta}{\alpha_c(A_{\max}-A_{\rm on})(\theta-A_{\rm on})}+\frac{1-e^{-\alpha_c\tau}}{\alpha_d(A_{\min}-A_{\rm off})}, \tag{15}$$

$$\frac{\partial P}{\partial A_{\rm off}}=\frac{1-e^{-\alpha_d\tau}}{\alpha_c(A_{\max}-A_{\rm on})}-\frac{\theta-A_{\min}}{(A_{\rm off}-\theta)(A_{\rm off}-A_{\min})}. \tag{16}$$

From this analysis we see that the amplitude variance does not depend on θ, while the period variance does. Since the amplitude increases as the bifurcation point is

approached, the relative amplitude fluctuations will decrease, as shown in Fig. 3(c). Furthermore, the critical behavior of the period is seen in the divergence of σ_P at the bifurcation point $\theta = A_{\rm off}$ in Eq. (16). A simple calculation shows that as $\theta \to A_{\rm off}$, $P \approx \ln(A_{\rm off} - \theta)$ and thus

$$\frac{\Delta P}{P} \approx \left[(A_{\rm off} - \theta) \ln \left[\frac{A_{\rm off} - A_{\rm min}}{A_{\rm off} - \theta} \right] \right]^{-1} . \tag{17}$$

Note that the argument of the logarithm is greater than one except when $\theta = A_{\rm min} = A_{\rm on}$. Our analysis thus predicts that as the point of oscillation onset is approached, the relative period fluctuations should increase rapidly, which is also in agreement with the data of Fig. 3(d).

2. SNF

In this section we first discuss problems involved with the analysis of fluctuations in the SNF case using standard theoretical approaches. We then justify our choice of which parameters fluctuate, and show how numerical integration of a simple stochastic DDE explains the observed stochastic behavior of the amplitude and period.

a. Additive and multiplicative noise. The behavior of ordinary differential equations (ODE's) near bifurcation points can be studied by looking at the extrema of the stationary probability density of the Fokker-Planck equation. These extrema are the quantities that undergo bifurcations. This is true for the Hopf bifurcation in ODE's, where other quantities such as the power spectrum and the autocorrelation function do not display this critical behavior.[17] For DDE's, the Fokker-Planck equation takes the form of a partial-differential equation with retarded argument. There are no analytical techniques available to solve such an equation for its stationary density. Further, to compute the density from an experimentally measured time series requires extensive data sets so the fluctuations can be averaged over many oscillation cycles.[17] Since our time series are short, such an approach would yield inaccurate results, expecially in regard to the position of the extrema of densities.

It is known that the relaxation time t_r of perturbations from the limit cycle (a measure of stability) is, according to Floquet theory,[18] given by $t_r \propto (n - n_0)^{-1}$, where n_0 is the parameter value at which the bifurcation occurs. This critical slowing down has been measured in the vicinity of the self-pulsing threshold of a bistable optical system governed by a DDE (the Ikeda equation).[19] The divergence of t_r is, along with $\tilde{A} \propto (n - n_0)^{1/2}$, characteristic of second-order phase transitions.[15] We cannot measure the relaxation time to the limit cycle because of the limit on the length of our data sets and the high noise levels. Even if we could measure this rate, it is not clear how to relate it to the amplitude and period fluctuations we are interested in. In view of this and of the problems involved with the density approach, we resort instead to numerical simulation. We apply noise to Eq. (3) since this equation is simpler than Eqs. (1) and (2) and explains qualitatively the deterministic behavior seen for SNF.[4]

To identify which parameters in Eq. (3) are subject to noise, we equate the asymptotes in the PCNF case (which we assumed are fluctuating) with the upper and lower bounds of the SNF function (see Fig. 6). This identification yields (setting $\alpha_c = \alpha_d$ for SNF)

$$c = -\frac{\gamma}{\beta} \ln \left[\frac{\phi_{\rm off} + \phi_b}{\phi_{\rm off}} \right] , \tag{18}$$

$$k = \alpha A_0 + \frac{\gamma}{\beta} \ln \left[\frac{\phi_{\rm off} + \phi_b}{\bar{\phi}} \right] , \tag{19}$$

and similar expressions if asymmetry (i.e., $\alpha_c \geq \alpha_d$) is kept. The physiological parameter that is probably fluctuating the most is γ since it is related to hippus. This is in agreement with earlier work showing that the amplitude of the noise depends on the state of the system, i.e., that the noise is multiplicative. In fact, it has been shown[8] that the neural output of the midbrain (which drives the iris constrictor muscle) is primarily the sum of two components: one proportional to light intensity and one proportional to both intensity and noise level. $\bar{\phi}$, related to the adaptation state of the retina, is also likely to fluctuate because of variations in light intensity.

It is obvious from Eqs. (18) and (19) that if either γ and/or $\bar{\phi}$ vary, c and k will also vary. Hence, the amplitude and period fluctuations in SNF should be qualitatively explained using Eq. (3) with additive noise (on k) and multiplicative noise (on c). When noise is assumed to affect γ and $\bar{\phi}$ in Eq. (2), it is considered multiplicative. If instead we use Eq. (3) with noise on c and k, we are assuming that the noise is both additive and multiplicative. *A priori,* this additive noise does not seem justified. However, additive noise is also expected in the general case [i.e., it could have been added to F in Eq. (2)], and could be due, for example, to random neuron firings in the absence of perturbations originating outside the reflex arc.

We assume colored Gaussian noise with a correlation time $t_{\rm corr} \approx 1$ sec (see Sec. III). Explicitly, we have $c = \bar{c} + \epsilon(t)$ (multiplicative noise) and $k = \bar{k} + \epsilon(t)$ (additive noise) where $\epsilon(t)$ obeys an Ornstein-Uhlenbeck process[15,20]

$$\frac{d\epsilon}{dt} = -\Gamma \epsilon(t) + \Gamma \xi(t) , \tag{20}$$

where $\Gamma \equiv t_{\rm corr}^{-1}$ and $\xi(t)$ is a Gaussian white noise of zero mean and variance σ^2, i.e., $\langle \xi(s)\xi(t) \rangle = \sigma^2 \delta(t-s)$. The correlation function of the Ornstein-Uhlenbeck process (20) is

$$C(t,s) = \frac{\sigma^2}{2t_{\rm corr}} e^{-\Gamma|t-s|} . \tag{21}$$

The white noise limit is obtained by letting $t_{\rm corr} \to 0$ in Eq. (21), and the strength of the Ornstein-Uhlenbeck noise is $\sigma^2 / 2t_{\rm corr}$.

b. Numerical algorithm. Stochastic simulations were done separately for additive and multiplicative noise.[21] The Ornstein-Uhlenbeck process (20) was integrated using an integral Euler method recently proposed by Fox *et al.*,[21] which has been shown to be more accurate than the usual differential method, while Eq. (3) was integrated using a fourth-order Runge-Kutta method with linear interpolation for the delay. The time step of $\tau/100$ was the

same for both methods and was limited by the accuracy requirements for the integration of the Ornstein-Uhlenbeck process. The parameters were chosen to be $\alpha=3.21$, $\tau=0.3$, $\bar{c}=200$, $\bar{k}=0$, and $\theta=50$ to yield reasonable pupil area values[11,14] in mm^2. The gain G in the SNF experiments is proportional to the parameter n, which controls the steepness of the Hill function at the fixed point. We varied n from its value at the Hopf bifurcation, $n_0=8.18$, to a value above which the amplitude grows very slowly ($n=12$). n was varied in steps of 0.02 from 8.18 to 8.30, and then by steps of 0.2 from 8.40 to 12.0.

Equation (3) was integrated using an initial function $A(t')=40$, $t'\in[-\tau,0]$, which is close to its deterministic fixed point ($A^*=44.6$). For a given value of n, the solution is first allowed to settle onto the limit cycle in the absence of noise for an integration time equal to 2500 delays; then noise is applied, and another 2500 delays are discarded as transients. Equation (3) is further integrated for another 20 000 delays during which the amplitude and period histograms are constructed. Periods and amplitudes were determined from the zero slope points of the solution as in the data analysis (Sec. III). We required two such points to be separated by at least 20 time steps (60 msec) in order to neglect very rapid changes in the derivative which could not be measured from the data.

It is difficult to numerically obtain an accurate description of steady-state behavior in the vicinity of a bifurcation point because of critical slowing down. Since the amplitude of the limit cycle at a Hopf bifurcation grows as $\tilde{A}\propto(n-n_0)^{1/2}$ and the relaxation time of transients onto the limit cycle goes as $t_r\propto(n-n_0)^{-1}$, it follows that $t_r\propto\tilde{A}^{-2}$. This implies that if we allow sufficient time for the transients to decay in the vicinity of the Hopf bifurcation point (i.e., for $n\approx n_0$), then this time should also be sufficient to obtain an accurate picture of the steady-state behavior for $n>n_0$. Hence, for all values of n, the same time (5000 delays) was allowed for the transients to decay. We have numerically verified that this transient period was sufficient by comparing our results in the vicinity of the Hopf bifurcation with those of simulations for 60 000 delays where the first 30 000 delays are discarded as transients.

A histogram of the amplitude values from the numerical solution of Eq. (3) with multiplicative noise on c given

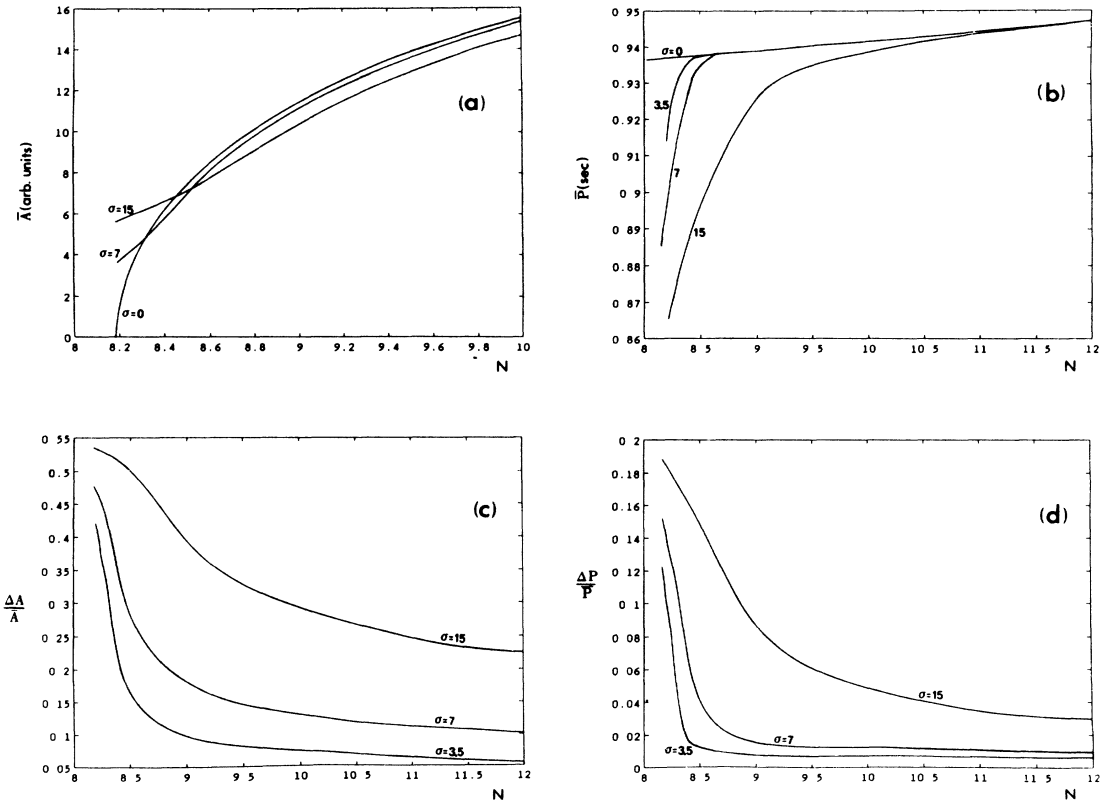

FIG. 4. Predicted means and fluctuations in amplitude and period for the SNF case, computed from the numerical integration of Eq. (3) with multiplicative Gaussian colored noise [Eq. (20)] on the parameter c. Parameter values are $\tau=0.3$ sec, $\bar{c}=200$ mm^2 sec^{-1}, $\theta=50$, $\alpha=3.21$ sec^{-1}, $k=0$ mm^2 sec^{-1}, and the initial area was constant (40 mm^2) on the interval $[-\tau,0]$. The bifurcation parameter is n (which is proportional to the feedback gain), and a Hopf bifurcation occurs at $n=8.18$. The noise correlation time is 1 sec. (a) Mean limit cycle amplitude as a function of n for the deterministic case ($\sigma=0$) and for $\sigma=7.0$ and 15.0. (b) Mean limit cycle period as a function of n for the deterministic case and for $\sigma=3.5,7.0,15.0$. (c) Relative amplitude fluctuations as a function of n for $\sigma=3.5$, 7.0, 15.0. (d) Relative period fluctuations for the same values of σ as in (c). Note that the mean period in (b) varies slowly with n, even though the expanded vertical scale suggests the opposite.

by Eq. (20) was obtained by dividing the interval (0,40) mm^2 into 200 bins. In Fig. 4(a), the mean amplitude calculated from this histogram is plotted as a function of the bifurcation parameter n for different intensities of the multiplicative noise ($t_{corr}=1$) as well as for the deterministic case. The curves were obtained by smoothing the simulation results at the discrete values of n. The mean amplitude in the presence of noise does not go to zero at the bifurcation as does the deterministic amplitude. This is in agreement with the observed behavior of the mean amplitude in Fig. 3(a). Rather, it levels off at a finite value proportional to the noise intensity. The sigmoidal shape of the curve for $\sigma=15$ is in good agreement with that of the experimental curve [Fig. 3(a)]. In this calculation, the very small amplitude fluctuations [corresponding to the first three bins of the amplitude histogram, equivalent to (0,0.6) mm^2] were neglected from the computation of the amplitude mean and standard deviation, to account for the fact that these small fluctuations are not measurable experimentally. The value at which the mean amplitude curve levels off at the bifurcation point is proportional to the number of low-amplitude bins neglected. Note that below the bifurcation point (i.e., for $n<n_0$), the mean amplitude is still finite, and goes to zero as the equilibrium point becomes more attracting (not shown).

The mean period is computed (as is the mean amplitude) from a histogram of the period values in the numerical solution of the stochastic DDE. The period value interval (0.5,1.5) sec was divided into 200 bins. The mean period value for the same range of noise intensities as in Fig. 4(a) is plotted in Fig. 4(b) as a function of n, as well as the period for the deterministic case. This plot shows that the mean period is fairly constant over the values of n investigated, as observed in the data [Fig. 3(b)]. In all cases, the period increases slightly with n; however, for a given value of n, the mean period decreases as the noise intensity increases.

For the PCNF case, it is possible to estimate the parameters of Eq. (4) from the PCNF data.[13] However, it is difficult to estimate the parameters of Eq. (3) from the SNF data, which is the reason why we are looking for qualitative agreement with the data in Fig. 3. The noise intensity was chosen to reproduce the values of relative amplitude and period fluctuations measured from the data [Figs. 3(c) and 3(d)]. Good agreement between these values and between the shape of the time series (not shown) was obtained when $\sigma=15$ [Figs. 4(c) and 4(d)]. This implies that the dependence of mean amplitude on n is given by the $\sigma=15$ curve in Fig. 4(a). This curve is in fact the one whose shape agrees the best with that of Fig. 3(a).

By repeating the simulations at a given value of n for the highest intensity used ($\sigma=15$), it was found that the mean and standard deviation values fluctuate by approximately 2%. This accuracy could be reduced by averaging these values over many realizations of the Ornstein-Uhlenbeck process. However, given the large variability exhibited by physiological systems, and given that we are looking for qualitative agreement, this averaging procedure was not warranted.

The simulations were repeated for the case of additive noise on k in Eq. (3). Note that c and k in Eq. (3) both determine the height of the SNF function. The results (not shown) are qualitatively the same as for the multiplicative case, except that for equal noise intensities, the additive noise has a lesser effect on the dynamics.

c. Pinpointing the Hopf bifurcation. Theoretically it is important to pinpoint the occurrence of the Hopf bifurcation. The fact that the mean limit cycle amplitude is still finite for $n<n_0$ might suggest that the bifurcation has occurred at a smaller parameter value than in the absence of noise. However, the onset of oscillation must be understood from the statistical behavior of the system. It has been shown that the stationary density of the Fokker-Planck equation corresponding to a generalized Langevin equation exhibits critical behavior, while other quantities such as the correlation function or the power spectrum do not exhibit such behavior.[15,17] A criterion for determining the Hopf bifurcation point in the presence of noise consists in finding the parameter value at which the stationary density goes from unimodal to bimodal. The separation of the peaks is proportional to the mean limit cycle amplitude which is different from the mean amplitude shown in Fig. 4(a). To distinguish between these two statistically determined amplitudes, the peak separation will be referred to as the *order parameter.*

The theory of invariant densities for delay-differential equations (DDE's), in general, and for stochastic DDE's, in particular, is nonexistent. Although the first-order DDE [Eq. (3)] is infinite dimensional (it evolves in a functional space), it might be appropriate to look at the one-dimensional density constructed from the values of the state variable. Histograms of the numerically computed solution of Eq. (3) with Eq. (20) for both the additive and multiplicative noise cases were constructed by dividing the interval (10,75) mm^2 of solution values into 500 bins. These histograms were found to have an invariant form when enough time was allowed for the transients to decay. This is an indication that these histograms may qualify as "invariant densities" for the DDE of interest. The peak separation was measured graphically from the densities. Again, repeated simulations for a fixed value of n revealed that peak separation values fluctuated by $\approx 5\%$ at the highest noise intensity used, and that the accuracy increased (the peaks were better defined) as n increased.

Figure 5 plots the magnitude of the order parameter as a function of the bifurcation parameter n for both multiplicative [Figs. 5(a) and 5(b)] and additive [Figs. 5(c) and 5(d)] noise. The computations were done on the same time series used for Fig. 4. In Figs. 5(a) and 5(c), the correlation time is fixed and the intensity varies over the same values as in Fig. 4. The curves are obtained by smoothing the simulation results at the discrete n values. Note that the deterministic curve is the same as that in Fig. 4(a): the amplitude is proportional to $(n-n_0)^{1/2}$ (Sec. IV B). The curves corresponding to finite noise intensities have the same shape as the deterministic curve but are shifted to its left (i.e., to higher values of n) by an amount proportional to the noise intensity. This implies that the noise actually postpones the Hopf bifurcation

(from the statistical point of view) in both the additive and multiplicative noise case.

In Figs. 5(b) and 5(d), the magnitude of the order parameter is again plotted as a function of n, but the noise intensity is fixed and the correlation time is varied from 1 to 4 sec. In both the additive and multiplicative case, the shift of the bifurcation point increases as the correlation time decreases.

V. TRANSITION FROM SNF TO PCNF

In this section the relation between the different deterministic properties of SNF and PCNF are investigated. Equation (3) can be obtained from Eqs. (1) and (2) by letting n go to infinity and by equating $A_{\text{off}}=(c+k)/\alpha$ and $A_{\text{on}}=k/\alpha$, as shown in Fig. 6. In this case, the forcing function F in Eq. (1) becomes a Heaviside function of the delayed pupil area. This limit produces a transition from the nearly sinusoidal oscillations in SNF to a switching type behavior, characteristic of relaxation oscillations, in PCNF.

The oscillation condition changes from Eq. (9) to the condition $(c+k)/\alpha>\theta$, where θ is the inflection point of the Hill's function when $n\to\infty$. This is illustrated in Fig. 6 where numerical solutions of Eq. (3) are plotted for different values of α. The PCNF waveform depends on the value of α at which the limit is taken. This depends on the intersection of the curve αA with the piecewise constant function. In the PCNF limit the inflection point of the Hill function becomes equal to θ. The oscillation condition is now that the intersection point be on the infinite slope portion of the PCNF function. Hence, in Fig. 6, when $\alpha=\alpha_1$, the condition $(c+k)/\alpha>\theta$ is not satisfied and there is no oscillation. When $\alpha=\alpha_2$ the limit produces a high-threshold oscillation, as in the case $\alpha=4$, and $\alpha=\alpha_4$ produces a low-threshold oscillation, as in the case $\alpha=0.7$.

For SNF the Hopf bifurcation criterion corresponds to a condition on the period involving the slope of the feedback function at the fixed point. For PCNF, the oscillation condition is a condition on the amplitude. In the SNF case at oscillation onset, the frequency is fixed while the amplitude is zero (in the supercritical case[4]), while in the PCNF case the amplitude is fixed while the frequency is zero. For SNF, once n increases past its value at the Hopf bifurcation, the amplitude first grows as $(n-n_0)^{1/2}$ but rapidly reaches its maximum value, i.e., that for the PCNF case.

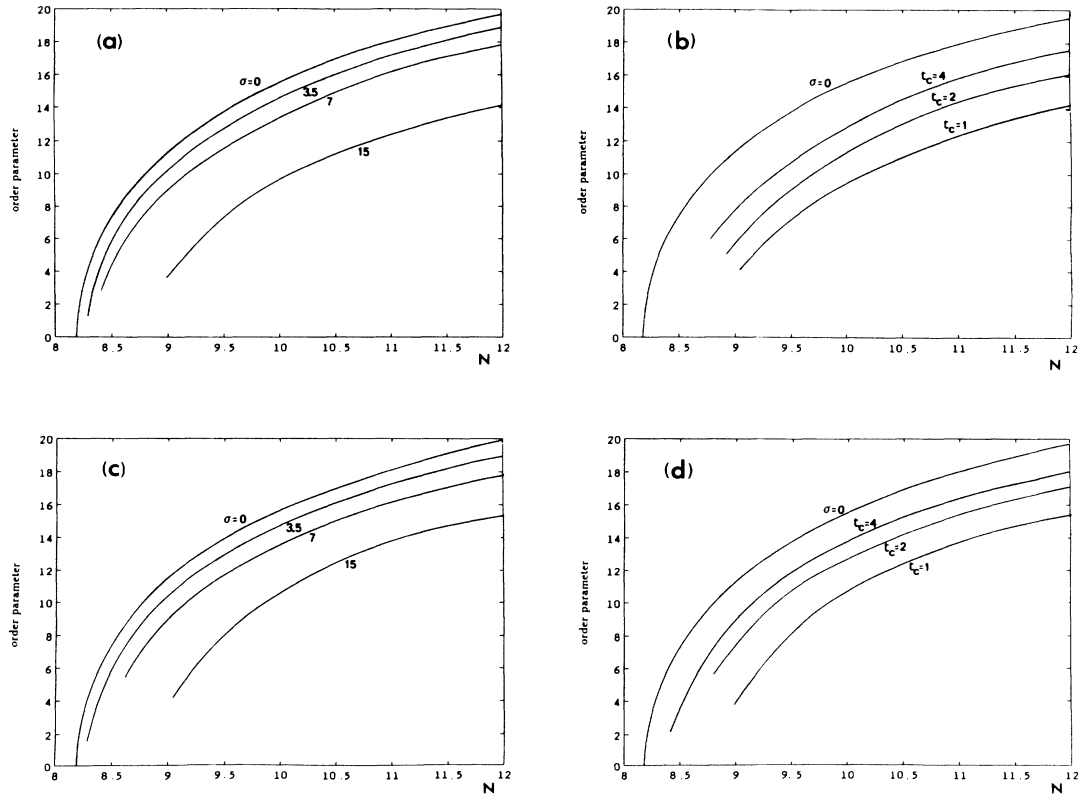

FIG. 5. Magnitude of the separation between the peaks (order parameter) in the density of the solution of Eq. (3) as a function of n for multiplicative [(a) and (b)] and additive [(c) and (d)] colored Gaussian noise [Eq. (20)]. The parameters are the same as in Fig. 4. In all plots, the amplitude of the limit cycle in the deterministic case is included for reference. (a) Peak separation for multiplicative noise of correlation time $t_{\text{corr}}\equiv t_c=1$ sec and for $\sigma=3.5$, 7.0, and 15.0. (b) Peak separation for multiplicative noise with $\sigma=15.0$ and for three different noise correlation times: $t_c=1.0$, 2.0, 4.0. (c) and (d) are the same as, respectively, (a) and (b), except that the noise is additive [on the parameter k in Eq. (3)].

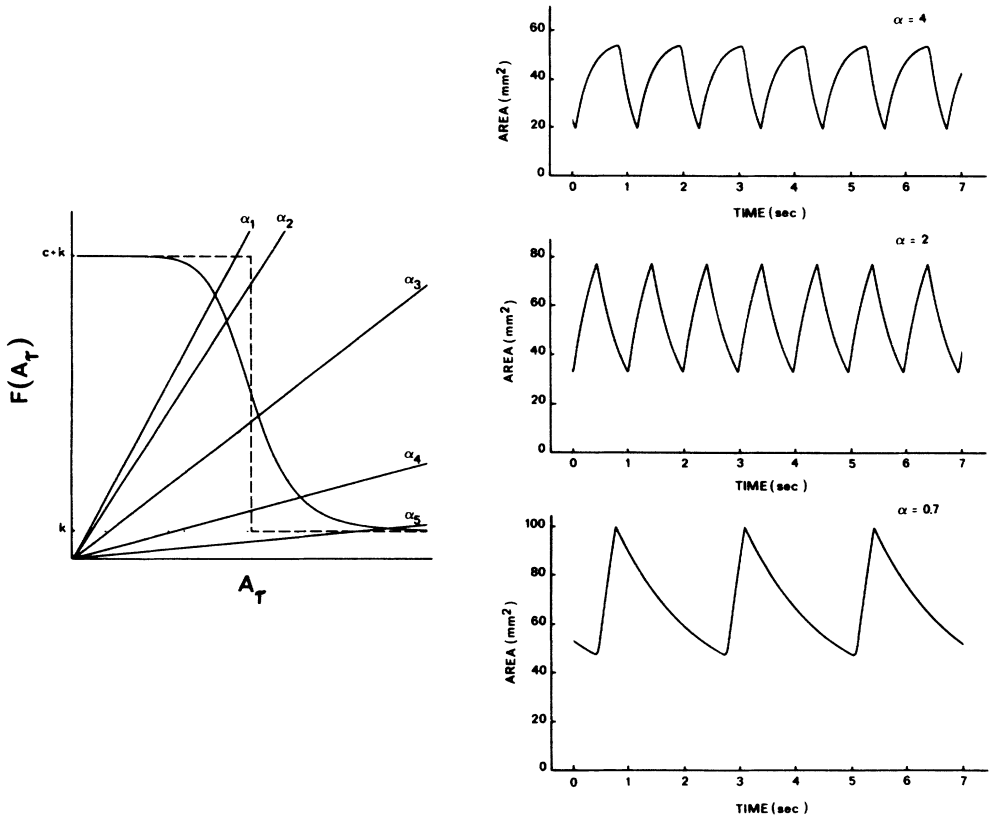

FIG. 6. Transition from SNF (solid line) to PCNF (dashed line) is achieved by increasing the slope of the feedback function until it approaches ∞ at θ and zero elsewhere [$\lim n \to \infty$ in the Hill's function on the left-hand side of Eq. (3)]. In this limit, the inflection point of the Hill's function coincides with θ, the upper bound $(c+k)/\alpha$ with the upper asymptote A_{off} and the lower bound k/α with A_{on}. Limit cycles bifurcate from the fixed point A^* of Eq. (3) when $\omega\tau \geq \cos^{-1}(-\alpha/\beta)$ [Eq. (9)]. In the PCNF limit, oscillation onset occurs when $\theta < A_{\text{off}}$. Depending on the value of α, the PCNF limit will yield solutions of Eq. (3) that either do not oscillate (α_1, α_5), or which oscillate around a high ($\alpha_2 = 4$) or a low ($\alpha_4 = 0.7$) threshold. Response asymmetry (i.e., $\alpha_c > \alpha_d$) observed in PCNF has been neglected for clarity. Parameters are $\tau = 0.3$, $n = 200$, $k = 20$, $c = 200$, $\theta = 50$, $\alpha = 3.21$, and the initial area was equal to 40.

VI. DISCUSSION

Oscillations in the human pupil light reflex were produced by two kinds of external electronic feedback which modify the normal functional dependence of retinal light flux on light intensity and pupil area. The parameters of the external feedback circuit were varied to induce a bifurcation from an equilibrium state to an oscillatory state: the gain of the amplifier relating light intensity to pupil area was varied in the SNF case, while the position of the threshold area θ was varied in the PCNF case.

Experimentally, it is observed that the period fluctuates more than the amplitude at oscillation onset in PCNF, while the opposite holds for the SNF case. We have related this to the different kind of critical behavior displayed by a first-order DDE at oscillation onset in the SNF and PCNF cases, under the assumption that the correlation time of the noise is of the same order or larger than the response time of the system. In fact, our simulations of Eq. (3) with multiplicative or additive noise (Fig. 4) indicate that this model of autonomous oscillations in pupil area qualitatively reproduces the observed behavior (Fig. 3) in the vicinity of oscillation onset.

Generally, relative amplitude fluctuations are greater than relative period fluctuations in SNF for a broad range of noise correlation times. Although our simulations account for the cycle-to-cycle fluctuations in period and amplitude in SNF, they do not reproduce the experimentally observed baseline drift over 10–15-sec periods [the data shown in Fig. 1(d) have been corrected for this drift]. This drift is probably due to an unmodeled deterministic phenomenon or to a noise source with a correlation time longer than that for the noise used in our simulations in Sec. IV B. This long-correlated noise could affect either c or k because a variation in either of these would result in a proportional variation in the mean value of the oscillation.

We have observed both experimentally and in our simulations that the period of SNF-induced pupillary oscillations remains constant despite variations in k, c, and n in the SNF case. The constancy of frequency in negative feedback systems in biology has been pointed out previously.[4,14,22] However, in the PCNF case, the period fluctuations are a consequence of the asymptote fluctuations (principally A_{off}). The theoretical result of Sec. IV B 1 for the amplitude and period fluctuations in PCNF

corresponds to an adiabatic elimination[15] in the sense that the system is considered to always be in a quasistationary state with respect to the instantaneous value of the fluctuating parameters.

The influence of the correlated noise in the PCNF case can also be qualitatively understood as follows. When pupil area approaches θ on the way to A_{off}, a slight fluctuation in A_{off} will affect the crossing time. Fluctuations in this crossing time are inversely proportional to the area derivative in the vicinity of the threshold. Hence near oscillation onset this derivative is nearly zero, making the period very sensitive to fluctuations in A_{off}. These conclusions hold under the hypothesis of colored multiplicative noise on the asymptotes. In the white noise limit both period and amplitude are sensitive to the noise (data not shown). However, in PCNF, as t_{corr} decreases, relative period and amplitude fluctuations are of the same order. In fact, whenever θ is approached, noise will cause transitions in pupil area from one side of the threshold to the other and back. Hence, the noise can shorten the time spent above θ, which will decrease the period and the amplitude. The fact that the amplitude fluctuations are not very large in PCNF is an indication that the noise in the pupil light reflex is colored.

Oscillation onset in PCNF does not correspond to a supercritical Hopf bifurcation as in the SNF case because the oscillation appears with a finite amplitude. Nor is it a subcritical Hopf bifurcation because the fixed point is globally asymptotically stable when $A_{\text{off}} < \theta$.[23] The difference lies in the exchange of stability that occurs at the bifurcation. As a supercritical Hopf bifurcation is approached, the stability of the fixed point decreases. Going through the bifurcation point, it becomes unstable and the solution is attracted to the limit cycle that came into existence at the bifurcation. In PCNF, the bifurcation is characterized by an abrupt exchange of stability leading to the appearance of an oscillation of infinite period but fixed amplitude. Closer inspection of the SNF-PCNF transition shows that oscillation onset is determined by a condition on the period in the SNF case (Hopf bifurcation criterion) and by one on the amplitude in the PCNF case ($A_i > \theta$, where A_i is the initial pupil area; or equivalently, $A_{\text{off}} > \theta$). It is interesting that in each case the assumed noise has less of an affect on the quantity which determines the oscillation condition (i.e., the noise does not effect the period as much as the amplitude in SNF, and vice versa in PCNF).

To identify whether a bifurcation has occurred or not in a physical system depends on which theory one uses. One such theory holds that a supercritical Hopf bifurcation occurs when the unique maximum of the stationary solution of the Fokker-Planck equation is replaced by two maxima which separate as the bifurcation parameter is increased. This does not mean that oscillations are not visible in the time series prior to the Hopf bifurcation. In fact, well-defined peaks in the power spectrum[24] as well as oscillations in the autocorrelation function appear, in the presence of noise, even when the bifurcation parameter is well below the deterministic bifurcation value.[17] But these quantities do not exhibit a qualitative change at some parameter alue. However, the probability density does display critical behavior. For physiological data, it is practically difficult to construct such a density due to the length of the available time series. Instead, we have made certain hypotheses on the noise sources and numerically simulated the stochastic dynamics of the system to see whether some aspects of the data can be reproduced. In this way, we were able to account for the observed behavior of period and amplitude fluctuations at oscillation onset.

In Fig. 5, it is shown that the bifurcation is shifted to higher values of the bifurcation parameter when noise is present. This postponement of the deterministic Hopf bifurcation in a DDE has not, to our knowledge, been reported previously, but is known to occur in ODE's when multiplicative noise is present.[15,17,25] We found the shift was proportional to the noise intensity σ, and inversely proportional to t_{corr}, as observed previously.[17]

A more surprising fact is that this shift also occurs for additive noise, with the same qualitative dependence on σ and t_{corr}. Noise-induced transitions due to additive noise are not possible in one dimension,[15] but they have been reported in a two-dimensional Fokker-Planck equation.[26] However, DDE's are infinite dimensional, and thus the possibility exists for such transitions. Further, shifts of the first transcritical bifurcation and of the first period-doubling bifurcation in the logistic map have been predicted and observed in numerical experiments involving additive and multiplicative noise.[27] In fact, for discrete time systems, there is an equivalence between additive and multiplicative noise.[27,28] Since the DDE reduces to such a map in the singular perturbation limit, where the response time of the system is much smaller than the delay,[29] it is not surprising that shifts occur for both additive and multiplicative noise.

The shift of the bifurcation point makes the application of the deterministic analysis to experimental data more difficult since a knowledge of the noise characteristics is needed to determine the deterministic bifurcation diagram. In view of the high noise levels in neural systems, it appears difficult to avoid this issue. More work is needed to determine the precise conditions under which postponements occur and whether advancements are possible.[17,25,30] In particular, other order parameters such as the root-mean-square amplitude may more appropriately describe the Hopf-type of time-translational symmetry-breaking bifurcation in the presence of noise studied here.[27,31] Also of interest is whether a two-dimensional stationary probability density is required to pinpoint the Hopf bifurcation, in the event where the radial and angular variables describing the oscillation are significantly coupled.[17,32] Natural coordinates in which to investigate this possibility are $A(t)$ and $A(t-\tau)$ in Eq. (3). Note that the shifts observed here are different from those obtained when the bifurcation parameter is swept at a finite rate across the bifurcation.[33]

The postponement of the Hopf bifurcation is expected to be qualitatively similar in the event that the fluctuations are not Gaussian distributed. Although we have not performed a precise assessment of noise statistics, the inclusion of Gaussian noise in our deterministic model does reproduce the data when given an adequate intensi-

ty. There have been previous reports[8] which support the Gaussian nature of the pupil noise for midrange pupil sizes under constant illumination. At large and small pupil sizes, the probability density of the noise is slightly skewed toward midrange values, presumably because the injected Gaussian noise is filtered by the nonlinearities in the motor pathway of this reflex. Our model would reproduce this behavior if the distribution of area values were computed prior to the Hopf bifurcation at small and large pupil sizes.

There have been previous studies of fluctuations in neuron membrane potential at rest[34] and at oscillation onset,[35] and in a simple motor task.[36] Here we have considered the onset of oscillation in a neural control system for which a simple, physiologically sound, model exists, and shown how this model can explain observed deterministic and stochastic behavior. We have further strived to identify the noise sources and to understand their dynamical behavior. Although a partly deterministic origin for the aperiodic behavior of the pupil (such as chaos) cannot be excluded, our results concerning the critical behavior of the pupil suggest that hippus is a reflection of an underlying stochastic process. Further, there does not seem to be any interaction between the dynamics of the noise source and the dynamics of the reflex, even though the pupil modifies the characteristics of the noise. This supports earlier hypotheses that the noise is injected into the reflex pathways.[8]

On the basis of our analysis, it is difficult to decide whether additive or multiplicative noise is responsible for the observed behavior of period and amplitude in SNF. Both mechanisms yield qualitatively similar results, and it is quite probable that both contribute to the observed behavior.

Noise is amplified in the SNF case near the Hopf bifurcation due to critical slowing down (loss of linear stability), which is responsible for the large amplitude fluctuations. In comparison, the PCNF case appears to be immune to this effect. The critical behavior is displayed by the mean period rather than the mean amplitude. This is interesting because it means that no noise amplification occurs at the bifurcation for PCNF. Instead the multiplicative noise causes period fluctuations and kicks the system between the limit cycle and fixed-point behaviors.

The SNF-PCNF limit has not, to our knowledge, been studied in DDE's. For the Ikeda equation in optical bistability,[37] another well-studied first-order DDE with nonlinear feedback, attention has been focused on the singular perturbation limit in which the ratio of the delay to the system response time goes to infinity [i.e., $\alpha\tau \gg 1$ in Eq. (3)]. Studies[29,38] have shown that certain properties of the map obtained in this limit carry over to the continuous solutions of the DDE, while others do not. This applies to the noisy DDE as well, since the noise is responsible for the bifurcation gap in the subharmonic cascade.[39] Also, a noisy one-dimensional map has been used in the study of noise-induced transitions between coexisting states of the Ikeda equation.[40] The PCNF limit of SNF yields a degenerate map with no interesting behavior. However, we have found (data not shown) that the mode frequencies obtained from a linear stability analysis converge to the odd harmonics of the fundamental mode as seen in the singular limit of the Ikeda equation.[38] Of course the mode amplitudes differ, since the singular limit produces a square wave while the PCNF limit produces the waveforms in Fig. 1(c).

Different methods are available for the analytical treatment of colored noise, depending on the ratio of system response time to noise correlation time.[15] If this ratio is large (the weakly colored noise case), the Fokker-Planck equation can be approximated using expansions in the inverse bandwidth of the noise. In the other case where the system is always at equilibrium with respect to the slowly varying noise, adiabatic elimination techniques (or switching-curve approximations[15]) can be used, as in Sec. IV B 1 for the PCNF case. In developing a quantitative analysis for autonomous oscillations in the pupil light reflex, one is faced with the problem that the noise correlation time (for the dominant noise components), the system response time and the delay are all of the same order of magnitude. This implies that the effect of noise on the dynamics may not be effectively studied using the aforementioned techniques. Further, it is not clear how to define the evolution of probability densities for DDE's. We expect that studies of other "untampered" or clamped neural control systems will face the same problems of equal time scales for noise, delay, and system response. Noise is an important component of neural activity, and it is our hope that this work will stimulate further studies to untangle the deterministic and stochastic contributions to neural oscillations. Further, the results reported here may be useful for the analysis of other experimental systems (e.g., in nonlinear optics, biochemical regulatory networks, Boolean kinetic networks, gene regulation and transcription) where noise is thought to play an important role and feedback dynamics can be modeled using smooth or piecewise linear nonlinearities.

ACKNOWLEDGMENTS

We are grateful to Hamamatsu Photonics Systems, Inc. (Hamamatsu City, Japan) for lending us their videopupillometer for these experiments. We are also grateful to Trevor Kirkham for his encouragement and to the Neuroelectronics group at the Montreal Neurological Institute for technical advice. One of us (A.L.) would like to thank the Natural Sciences and Engineering Research Council (Canada) for financial support.

*Present address: Theoretical Division B-213, Los Alamos National Laboratory, Los Alamos, NM 87545.

†Present address and to whom reprint requests should be directed: Department of Neurology, Box 425, The University of Chicago Hospitals, 5841 South Maryland Avenue, Chicago, IL 60637.

[1] M. C. Mackey and L. Glass, Science **197**, 287 (1977); L. Glass and M. C. Mackey, Ann. N. Y. Acad. Sci. **316**, 214 (1979).

[2]M. C. Mackey and J. G. Milton, Ann. N. Y. Acad. Sci. **504**, 16 (1987).
[3]J. G. Milton, A. Longtin, A. Beuter, M. C. Mackey, and L. Glass, J. Theor. Biol. **138**, 129 (1989).
[4]A. Longtin and J. G. Milton, Bull. Math. Biol. **51**, 605 (1989).
[5]L. Stark, IEEE Trans. Biomed. Eng. **31**, 919 (1984).
[6]L. Stark and T. N. Cornsweet, Science **127**, 588 (1958).
[7]L. Stark, F. W. Campbell, and J. Atwood, Nature **182**, 857 (1958); L. Stark, Proc. IRE **47**, 1925 (1959).
[8]S. F. Stanten and L. Stark, IEEE Trans. Biomed. Eng. **13**, 140 (1966); S. Usui and L. Stark, Biol. Cybern. **45**, 13 (1982).
[9]L. Stark and P. M. Sherman, J. Neurophysiol. **20**, 17 (1957).
[10]L. Stark, J. Opt. Soc. Am. **52**, 925 (1962).
[11]A. Longtin and J. G. Milton, Math. Biosci. **90**, 183 (1988).
[12]J. P. H. Reulen, J. T. Marcus, M. J. van Gilst, D. Koops, J. E. Bos, G. Tiesinga, F. R. de Vries, and K. Boshuizen, Med. Biol. Eng. Comp. **26**, 27 (1988).
[13]J. G. Milton and A. Longtin, Vision Res. **30**, 515 (1990); J. G. Milton, A. Longtin, T. H. Kirkham, and G. S. Francis, Am. J. Ophthalmol. **105**, 402 (1988).
[14]A. Longtin and J. G. Milton, Biol. Cybern. **61**, 51 (1989).
[15]W. Horsthemke and R. Lefever, *Noise Induced Transitions: Theory and Applications in Physics, Chemistry and Biology,* Vol. 15 of *Springer Series in Synergetics,* edited by H. Haken (Springer, Berlin, 1984).
[16]J. Guckenheimer and P. Holmes, *Nonlinear Oscillations, Dynamical Systems, and Bifurcations of Vector Fields* (Springer, New York, 1983).
[17]L. Fronzoni, R. Mannella, P. V. E. McClintock, and F. Moss, Phys. Rev. A **36**, 834 (1987).
[18]G. Iooss and D. D. Joseph, *Elementary Stability and Bifurcation Theory* (Springer, New York, 1980).
[19]J. Y. Gao, J. M. Yuan and L. M. Narducci, Opt. Commun. **44**, 201 (1983).
[20]C. W. Gardiner, *Handbook of Stochastic Methods for Physics, Chemistry and the Natural Sciences* (Springer, Berlin, 1985).
[21]R. F. Fox, J. Stat. Phys. **46**, 1145 (1987); R. F. Fox, I. R. Gatland, R. Roy, and G. Vemuri, Phys. Rev. A **38**, 5938 (1988); J. M. Sancho, M. San Miguel, S. L. Katz, and J. D. Gunton, *ibid.* **26**, 1589 (1982).
[22]P. E. Rapp, A. I. Mees, and C. T. Sparrow, J. Theor. Biol. **90**, 531 (1981).
[23]U. an der Heiden and M. C. Mackey, J. Math. Biol. **16**, 75 (1982).
[24]K. Wiesenfeld, J. Stat. Phys. **38**, 1071 (1985).
[25]R. Lefever and J. Wm. Turner, Phys. Rev. Lett. **56**, 1631 (1986); S. Kabashima and T. Kawakubo, Phys. Lett. **70A**, 375 (1979).
[26]L. Schimansky-Geier, A. V. Tolstopjatenko, and W. Ebeling, Phys. Lett. **108A**, 329 (1985).
[27]S. J. Linz and M. Lücke, Phys. Rev. A **33**, 2694 (1986).
[28]J. P. Crutchfield, J. D. Farmer, and B. A. Huberman, Phys. Rep. **92**, 45 (1982).
[29]J. Mallet-Paret and R. D. Nussbaum, in *Chaotic Dynamics and Fractals,* edited by M. F. Barnsley and S. G. Demko (Academic, Orlando, 1986); J. Y. Gao, L. M. Narducci, L. S. Schulman, M. Squicciarini, and J. M. Yuan, Phys. Rev. A **28**, 2910 (1983); J. Y. Gao, L. M. Narducci, H. Sadiky, M. Squicciarini, and J. M. Yuan, *ibid.* **30**, 901 (1984).
[30]A. Longtin and M. C. Mackey (unpublished).
[31]P. C. Martin, in *Melting, Localization and Chaos,* edited by R. K. Kalia and P. Vashista (North-Holland, Amsterdam, 1982), p. 179.
[32]M. San Miguel and S. Chaturvedi, Z. Phys. B **40**, 167 (1980).
[33]L. Fronzoni, F. Moss, and P. V. E. McClintock, Phys. Rev. A **36**, 1492 (1987); S. M. Baer, T. Erneux, and J. Rinzel, Siam. J. Appl. Math. **49**, 55 (1989).
[34]C. Stevens, in *Membranes, Ions and Impulses,* edited by J. W. Moore (Plenum, New York, 1975).
[35]G. Matsumoto, I. Tasaki, and I. Inoue, J. Phys. Soc. Jpn. **44**, 351 (1978); G. Matsumoto and T. Kunisawa, *ibid.* **44**, 1047 (1978).
[36]H. Haken, J. A. S. Kelso, and H. Bunz, Biol. Cybern. **51**, 347 (1985).
[37]K. Ikeda, Opt. Commun. **39**, 257 (1979).
[38]P. Nardone, P. Mandel, and R. Kapral, Phys. Rev. A **33**, 2465 (1986).
[39]M. W. Derstine, H. M. Gibbs, F. A. Hopf, and D. L. Kaplan, Phys. Rev. A **26**, 3720 (1982); R. Vallée, C. Delisle, and J. Chrostowski, *ibid.* **30**, 336 (1984).
[40]R. Kapral, E. Celarier, P. Mandel, and P. Nardone, SPIE Optical Chaos **667**, 175 (1986).